

Phase-space measurements and decoherence for angular momentum systems

DORJE C. BRODY¹, EVA-MARIA GRAEFE², AND RISHINDRA MELANATHURU²

¹*School of Mathematics and Physics, University of Surrey, Guildford GU2 7XH, UK*

²*Department of Mathematics, Imperial College London, London SW7 2AZ, UK*

The monitoring of the three independent components of the angular momentum (or spin) of a quantum system by its environment that does not isolate any preferred orientation is modelled in two different ways. One describes the dynamics by the Lindblad equation generated by three independent angular momentum operators. The other uses iterated measurements of the “phase-space” point on the sphere in terms of the positive operator-valued measure generated by SU(2) coherent states. In contrast to the equivalent scenario on a flat phase space, these two models give rise to subtle differences. Specifically, it is shown that the two super-operators corresponding to the two decoherence models for angular momentum systems are commutative, but their eigenvalues are different. Hence although both models give rise to phase-space decoherence, their dynamical behaviours are not equivalent. In either model, we find that the characterisation of classicality as represented by the decay rates of the elements of the density matrix (i.e. decoherence) and that as represented by the positivity of the quasiprobability distribution are not equivalent for angular momentum systems.

I. INTRODUCTION

The loss of quantum coherence in the phase space of a quantum system can be modelled by assuming that the environment simultaneously monitors independent components of the system’s phase-space variables [1]. This differs fundamentally from the more familiar decoherence models arising from the monitoring of a single observable such as the position [2–5], which, while often investigated in phase space [6–9], need not suppress all quantum interference effects on phase space. In contrast, a phase-space decoherence model necessarily eliminates quantum interference effects on phase space entirely [1].

A natural dynamical framework that captures the effect of a monitoring of observables in continuous time is the Lindblad equation [10–12], driven by these independent observables. For instance, for a quantum system defined on the real line (or in two- or three-dimensional space), the relevant phase-space variables are the position and momentum. In this case, phase-space decoherence can be modelled by a Lindblad equation with Lindblad operators given by the position and momentum observables themselves [1, 13, 14]. It has been shown in [1] that the effect of such Lindbladian dynamics on the system is equivalent to that of repeated measurements of the phase-space coordinates described by the positive operator-valued measure (POVM) associated with coherent states. That is, the Lindblad equation can be unravelled by means of repeated phase-space POVM measurements. The outcome of each POVM measurement is a phase-space point, and the resulting state is a coherent state centred at that point. More generally, if the system is monitored by the environment, then we have a nonselective measurement, and the outcome state is the projection operator onto a coherent state, averaged over the phase space with respect to the Husimi distribution of the initial state. This process can be iterated successively to yield nontrivial state transformations, because no two

outcome states can be orthogonal. The equivalence with the Lindbladian dynamics driven by position and momentum can be deduced from the fact that the solution to the Lindblad equation at the discrete times $t_k = \lambda k$, with $k = 0, 1, 2, \dots$, for a suitable constant $\lambda > 0$, agrees with the outcome states of k successive POVM measurements [1]. This is perhaps expected, given that both schemes model measurements of the phase-space location of the system.

In the present paper we investigate an analogous situation for quantum systems described in terms of angular momentum operators, where the phase space is spherical. Specifically, we consider a Lindblad evolution modelling the simultaneous continuous measurement of the three orthogonal angular momentum components, in comparison to the effect of successive POVM measurements with respect to spin coherent states. Given the equivalence of the two models in the case of a flat phase space, and the intimate connection of both the Lindblad dynamics and the coherent states to the heat equation [15], one might expect the two phase-space decoherence models to agree. However, by deriving explicit solutions for the time-dependent density operator in both models, expanded in terms of the spin-moment components, we reveal a discrepancy between the two descriptions. While both models lead to the expected decoherence effect of dampening the off-diagonal elements of the density matrix and driving it eventually to the state of complete ignorance, we find that the decay rates of each of the moments are different (with the exceptions of spin- $\frac{1}{2}$ systems). The qualitative effects of both phase-space decoherence models are equivalent, yet the difference in the decay rates should be experimentally measurable, allowing an experimental investigation into whether either of the two models introduced here might capture the effect of an environment that does not isolate any preferred spin orientation.

The paper is organised as follows. In Section II we

investigate the continuous-time phase-space decoherence model given by the Lindblad equation for the density matrix, and present the solution. In Section III we compare this to the effect of phase-space POVM measurements on the density matrix. In Section IV we compare the corresponding decoherence rates for the two decoherence models, and show that in general they do not agree. In Section V we recast these results in terms of phase-space quasidistribution functions, working out explicit representations of the solution to the dynamical equation. We conclude in Section VI with a brief summary and discussion.

II. CONTINUOUS-TIME SPIN MONITORING

For the purpose of modelling the continuous-time monitoring of the three independent spin components by the environment, let us consider an angular momentum system whose state obeys the Lindblad equation

$$\frac{d\hat{\rho}}{dt} = \gamma \left(\hat{J}_x \hat{\rho} \hat{J}_x + \hat{J}_y \hat{\rho} \hat{J}_y + \hat{J}_z \hat{\rho} \hat{J}_z - \frac{1}{2} \left(\hat{J}_x^2 \hat{\rho} + \hat{\rho} \hat{J}_x^2 \right) - \frac{1}{2} \left(\hat{J}_y^2 \hat{\rho} + \hat{\rho} \hat{J}_y^2 \right) - \frac{1}{2} \left(\hat{J}_z^2 \hat{\rho} + \hat{\rho} \hat{J}_z^2 \right) \right), \quad (1)$$

where $\gamma > 0$ is a parameter that determines the decoherence rate, and the three spin operators \hat{J}_x , \hat{J}_y , and \hat{J}_z driving the dynamics satisfy the usual $SU(2)$ commutation relations $[\hat{J}_x, \hat{J}_y] = i\hat{J}_z$, $[\hat{J}_y, \hat{J}_z] = i\hat{J}_x$, and $[\hat{J}_z, \hat{J}_x] = i\hat{J}_y$. This Lindblad equation has been investigated in the literature in the context of depolarisation dynamics [16]. It can be derived, for example, using a microscopic model of a spin interacting with a fluctuating magnetic field [17], but also based on other setups [18–20]. (In Appendix A we provide another derivation of a microscopic model of a particle in an environment that monitors its angular momentum components.) An alternative way of expressing the dynamical equation is to use the spin raising and lowering operators $\hat{J}_{\pm} = \hat{J}_x \pm i\hat{J}_y$. In terms of these operators, the dynamical equation (1) can be expressed in the form

$$\frac{d\hat{\rho}}{dt} = \gamma \left(\frac{1}{2} \hat{J}_+ \hat{\rho} \hat{J}_- + \frac{1}{2} \hat{J}_- \hat{\rho} \hat{J}_+ + \hat{J}_z \hat{\rho} \hat{J}_z - J(J+1)\hat{\rho} \right). \quad (2)$$

Although the solution to the dynamical equation (1) is known in the literature (see [17] and references cited therein), we shall derive it here so that comparison with the POVM measurement becomes more transparent. To solve the Lindblad equation we find it convenient to use irreducible tensor operators $\{\hat{T}_{L,k}^J\}$, which constitute a suitable basis for analysing spin systems [21–23]. These operators satisfy the commutation relations

$$[\hat{J}_z, \hat{T}_{L,k}^J] = k \hat{T}_{L,k}^J \quad (3)$$

and

$$[\hat{J}_{\pm}, \hat{T}_{L,k}^J] = \sqrt{(L \mp k)(L \pm k + 1)} \hat{T}_{L,k \pm 1}^J, \quad (4)$$

and form a Hilbert-Schmidt orthonormal operator basis in the sense that

$$\text{tr} \left(\hat{T}_{L,k}^J (\hat{T}_{L',k'}^J)^\dagger \right) = \delta_{LL'} \delta_{kk'}, \quad (5)$$

where $(\hat{T}_{L,k}^J)^\dagger = (-1)^k \hat{T}_{L,-k}^J$. The index L runs from 0 to $2J$, while k runs from $-L$ to L . The index J on the other hand is fixed, and acts as a placeholder to indicate the total spin of the system. As an example, for a spin-1 system, we have the nine basis elements

$$\hat{T}_{0,0}^1 = \frac{1}{\sqrt{3}} \mathbb{1}, \quad (6)$$

$$\hat{T}_{1,0}^1 = \frac{1}{\sqrt{2}} \hat{J}_z, \quad (7)$$

$$\hat{T}_{1,\pm 1}^1 = \mp \frac{1}{2} \hat{J}_{\pm}, \quad (8)$$

$$\hat{T}_{2,0}^1 = \frac{1}{\sqrt{6}} (3\hat{J}_z^2 - \hat{J}^2), \quad (9)$$

$$\hat{T}_{2,\pm 1}^1 = \mp \frac{1}{2} (\hat{J}_{\pm} \hat{J}_z + \hat{J}_z \hat{J}_{\pm}), \quad (10)$$

$$\hat{T}_{2,\pm 2}^1 = \frac{1}{2} \hat{J}_{\pm}^2. \quad (11)$$

These can be used to expand any 3×3 observable. More generally, the matrix elements of the irreducible tensors in the standard \hat{J}_z -bases are given by

$$\langle J, m' | \hat{T}_{L,k}^J | J, m \rangle = \sqrt{\frac{2L+1}{2J+1}} C_{JmLk}^{Jm'}, \quad (12)$$

where the $C_{j_1 m_1 j_2 m_2}^{J M}$ denote the Clebsch-Gordan coefficients.

In terms of the irreducible tensor operators the initial state of the system can be expanded according to

$$\hat{\rho} = \sum_{L=0}^{2J} \sum_{k=-L}^L \rho_{Lk} \hat{T}_{L,k}^J, \quad \rho_{L,k} = \text{tr} \left((\hat{T}_{L,k}^J)^\dagger \hat{\rho} \right). \quad (13)$$

The expansion coefficients are often referred to as the monopole moment for ρ_{00} , the vector moments or orientations for ρ_{1k} , $k = -1, 0, 1$, the quadrupole moment or alignment for ρ_{2k} , $k = -2, \dots, 2$, and so on [24, 25].

What makes the irreducible tensor operator basis particularly well suited for our purposes is that the $\{\hat{T}_{L,k}^J\}$ are eigenoperators of the Lindblad equation (1). Specifically, writing the right side of (1) in the form

$$\mathcal{L}(\hat{\rho}) = -\frac{1}{2} \gamma \sum_{i=x,y,z} [\hat{J}_i, [\hat{J}_i, \hat{\rho}]], \quad (14)$$

we have (see [22, 23])

$$\mathcal{L}(\hat{T}_{L,k}^J) = -\frac{1}{2} \gamma L(L+1) \hat{T}_{L,k}^J. \quad (15)$$

It then follows that the solution to (1) is

$$\hat{\rho}_t = \sum_{L=0}^{2J} \sum_{k=-L}^L e^{-\frac{1}{2} \gamma L(L+1)t} \rho_{Lk} \hat{T}_{L,k}^J, \quad (16)$$

where ρ_{Lk} are the components of the initial density matrix defined in (13). We see therefore that the effect of phase-space decoherence is to exponentially damp the elements of the density matrix. In particular, in the large time limit, only the $L = k = 0$ term in the sum (16) survives, and from $\hat{T}_{0,0}^J = \frac{1}{\sqrt{2J+1}}\mathbb{1}$ we thus see that $\hat{\rho}_t$ converges asymptotically to the state of complete ignorance.

III. COHERENT-STATE POVM MEASUREMENTS

As an alternative to the Lindblad dynamics, one can model the effects of phase-space measurements with an application of a sequence of coherent-state POVMs [26, 27]. Under such a POVM, if we start from an arbitrary initial state $\hat{\rho}$ of a spin- J system and perform a measurement of the phase-space point of the system on the sphere, then the output state when the measurement outcome is recorded is given by the spin- J coherent state centred at that point. In terms of the complex parameterisation $z = \tan(\frac{\theta}{2}) \exp(i\phi)$ for points on phase space, where θ and ϕ are the usual spherical coordinates, the coherent state is given by [28–32]:

$$\begin{aligned} |z\rangle &= (1 + |z|^2)^{-J} e^{z\hat{J}_-} |J, J\rangle \\ &= (1 + |z|^2)^{-J} \sum_{k=-J}^J \sqrt{\binom{2J}{J+k}} z^{J-k} |J, k\rangle. \end{aligned} \quad (17)$$

Here $\{|J, k\rangle\}_{k=-J}^J$ is the eigenbasis of \hat{J}_z . The coherent states $|z\rangle$ form an overcomplete basis of the Hilbert space, with the resolution of the identity

$$\int |z\rangle\langle z| d\mu_{\theta,\phi}^J = \mathbb{1}, \quad (18)$$

where

$$d\mu_{\theta,\phi}^J = \frac{2J+1}{4\pi} \sin\theta d\theta d\phi \quad (19)$$

denotes the spherical measure over the spin phase space [33]. In this measurement the probability of detecting a phase-space event [34, 35] in a region A of the phase space is given by

$$\mathbb{P}(z \in A) = \int_A \langle z|\hat{\rho}|z\rangle d\mu_{\theta,\phi}^J. \quad (20)$$

If the phase-space coordinates (i.e. the direction of the spin) are monitored by the environment, then no outcome is recorded, and the state of the system decoheres. In particular, writing $\hat{\rho}^{(1)}$ for the outcome state of the system after a single POVM measurement, we have

$$\hat{\rho}^{(1)} = \int \langle z|\hat{\rho}|z\rangle |z\rangle\langle z| d\mu_{\theta,\phi}^J. \quad (21)$$

To compare the effect of the POVM measurement with the solution (16) to the Lindblad equation, we shall begin by showing that the irreducible tensor operators, as well as being eigenstates of the Lindblad operators, are simultaneous eigenstates of the POVM operation. That is, writing

$$\Phi[\hat{A}] = \int \langle z|\hat{A}|z\rangle |z\rangle\langle z| d\mu_{\theta,\phi}^J \quad (22)$$

for any operator \hat{A} , we have $\Phi[\hat{T}_{L,k}^J] \propto \hat{T}_{L,k}^J$. To show this, we expand the coherent state projector in terms of $(\hat{T}_{L,k}^J)^\dagger$ by writing

$$|z\rangle\langle z| = \sum_{L=0}^{2J} \sum_{k=-L}^L \overline{c_{L,k}(z)} (\hat{T}_{L,k}^J)^\dagger, \quad (23)$$

where $c_{L,k}(z) = \langle z|(\hat{T}_{L,k}^J)|z\rangle$. The expansion coefficients admit the representation [21, 29, 30, 36]

$$c_{L,k}(z) = \frac{1}{\sqrt{2J+1}} \left[\frac{\binom{2J}{L}}{\binom{2J+L+1}{L}} \right]^{\frac{1}{2}} Y_L^k(\theta, \phi) \quad (24)$$

where $Y_L^k(\theta, \phi)$ denotes the spherical harmonics [21, 23, 37–39], satisfying the orthonormality condition¹

$$\int Y_{L_1}^{k_1} \overline{Y_{L_2}^{k_2}} d\mu_{\theta,\phi}^0 = \delta_{L_1 L_2} \delta_{k_1 k_2}. \quad (25)$$

Hence the map

$$\Phi[\hat{T}_{L,k}^J] = \int |z\rangle\langle z| \hat{T}_{L,k}^J |z\rangle\langle z| d\mu_{\theta,\phi}^J \quad (26)$$

on $\hat{T}_{L,k}^J$ involves integration over a pair of spherical harmonics, which on account of the orthogonality relation (25) simplifies to give

$$\Phi[\hat{T}_{L,k}^J] = \frac{\binom{2J}{L}}{\binom{2J+L+1}{L}} \hat{T}_{L,k}^J. \quad (27)$$

Thus the operators $\hat{T}_{L,k}^J$ form eigenstates of the POVM map Φ with the eigenvalues given by the ratio of binomial coefficients in (27).

Equipped with this result, we are able to determine the effect of a phase-space POVM measurement on an arbitrary initial state $\hat{\rho}$. Specifically, expanding $\hat{\rho}$ in the form (13) we find at once that after the application of a

¹ We use the convention $Y_0^0 = 1$, so that the spherical harmonics are orthonormal with respect to the uniform probability measure $d\mu_{\theta,\phi}^0 = (4\pi)^{-1} \sin\theta d\theta d\phi$. This differs from the Condon–Shortley convention by a factor of $\sqrt{4\pi}$: $Y_L^m = \sqrt{4\pi} Y_L^{m,\text{CS}}$, or equivalently $Y_L^m = \sqrt{2L+1} Y_L^{m,\text{Racah}}$, where $Y_L^{m,\text{Racah}} = (-1)^m \sqrt{(L-m)!/(L+m)!} P_L^m(\cos\theta) e^{im\phi}$ for $m \geq 0$.

single measurement the expansion coefficients transform according to

$$\rho_{Lk} \rightarrow \left[\frac{\binom{2J}{L}}{\binom{2J+L+1}{L}} \right] \rho_{Lk}. \quad (28)$$

It also follows, more generally, that an application of n successive measurements will transform the state into

$$\hat{\rho}^{(n)} = \sum_{L=0}^{2J} \sum_{k=-L}^L \left[\frac{\binom{2J}{L}}{\binom{2J+L+1}{L}} \right]^n \rho_{Lk} \hat{T}_{L,k}^J. \quad (29)$$

Analogous to the solution (16) to the Lindblad dynamics, the off-diagonal elements of the density matrix are exponentially suppressed, and the state eventually decays into the stable state $\rho_{00} \hat{T}_{0,0}^J = \frac{1}{2J+1} \mathbf{1}$, the state of complete ignorance.

IV. COMPARISON OF THE DECOHERENCE RATES

Although the two models of phase-space decoherence give rise to the same asymptotic results, the decoherence rates are not identical. Specifically, the decay rates for the Lindblad process are given by

$$\Gamma_L^{(\text{Lind})} = \frac{1}{2} \gamma L(L+1), \quad (30)$$

while the corresponding decay rates of the sequence of POVM measurements, when we view the iteration count n as representing time, are given by

$$\Gamma_L^{(\text{POVM})} = -\log \left(\frac{\binom{2J}{L}}{\binom{2J+L+1}{L}} \right). \quad (31)$$

Both decay rates are independent of the value of k . While in both cases $\Gamma_0 = 0$, the decay rates for the other $L \neq 0$ components differ in general, except in the case $J = 1/2$. For $J = 1/2$ there is only one nonzero decay rate in both cases, and they agree under the choice $\gamma = \log 3$. In this case the solution to the Lindblad equation at $t = n$ agrees with the outcome state resulting from n iterated POVM measurements.

The behaviours of the two models become analogous also for large spins in the following sense. When L is held fixed, for large spin J we have

$$\Gamma_L^{(\text{POVM})} \approx \frac{1}{2J} L(L+1) - \frac{1}{4J^2} L(L+1) + \frac{1}{48J^3} L(L+1)(L^2 + L + 6), \quad (32)$$

and hence $\Gamma_L^{(\text{POVM})} \rightarrow \Gamma_L^{(\text{Lind})}$ if we let $\gamma = 1/J$. However, if L scales with J , and recall that L ranges from 0 to $2J$, then the decay rates do not agree. Nevertheless, in this case the large- L components of the density matrix in either model will decay so fast anyhow that they

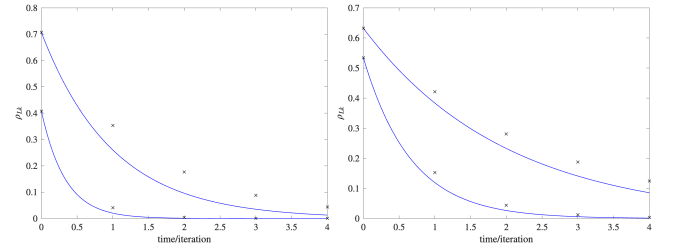


FIG. 1: Decoherence effect for $J = 1$ (left) and $J = 5$ (right). The components ρ_{20} and ρ_{10} of the density matrix, prepared initially in a coherent state, as functions of time/iteration number for the Lindblad dynamics (solid blue lines, with $\gamma = 1/J$) and repeated POVM measurements (black crosses) are shown here. The impact of decoherence in terms of the decay of the elements of the density matrix is less pronounced with coherent states having larger spins.

will make little practical difference. In this sense the two models behave similarly for large spins. For intermediate spins, the two decoherence models are not equivalent, although their dynamical characteristics agree qualitatively, and in the asymptotic limits $t \rightarrow \infty$ and $n \rightarrow \infty$ the off-diagonal terms are suppressed, while the diagonal elements approach a uniform distribution, independently of the choice of the basis in which the density matrix is represented.

The existence of the two distinct yet plausible models for the decoherence arising from an isotropic environmental monitoring of the spin raises the question of whether a physical environment might preferentially follow one over the other (or follow a third option). To distinguish the dynamics identified here in a possible experiment, one could examine the relative decay of different multipole moments. Recall that we are comparing decoherence models with two decay rates (30) and (31). For $L = 1, 2$ (dipole and quadrupole sectors), the corresponding decay rates do not coincide. In Figure 1 we display examples of both the POVM and the Lindblad dynamics, for an initial coherent state pointing towards the north pole (“spin up”) for $J = 1$ and $J = 5$, respectively, where we have set $\gamma = 1/J$ for the parameter in the Lindblad dynamics. Specifically, the components ρ_{Lk} of the density matrix for $L = 1, 2$ and $k = 0$ for both the Lindblad evolution (solid blue lines) and iterated POVMs (denoted by black crosses) are shown. For both values of J the decay of these elements is visibly different between the two models. In general, the value of γ is arbitrary, so it is better to consider ratios of decay rates. For spin-1, for example, we find

$$\frac{\Gamma_2^{(\text{Lind})}}{\Gamma_1^{(\text{Lind})}} = 3 \quad \text{and} \quad \frac{\Gamma_2^{(\text{POVM})}}{\Gamma_1^{(\text{POVM})}} = \frac{\log 10}{\log 2} \approx 3.32. \quad (33)$$

These dimensionless numbers provide a subtle discrimination between the two models.

These decay rates can be accessed from monitoring the so-called orientation sector ρ_{1k} and the alignment sector ρ_{2k} . These are the coefficients of the spin-1 density ma-

trix in the irreducible tensor basis [40–45]). In an experimental setting where it is expected that an environment monitors the spin without isolating a preferred orientation (for a generic environment, a symmetry argument requires that no orientation should be preferred), one could empirically determine which model is more representative by measuring $\rho_{1k}(t)$ and $\rho_{2k'}(t)$ after some time t , having prepared the initial state of the system in some $\rho_{Lk}(0)$, and forming the empirical ratio

$$R = \frac{\log(|\rho_{2k'}(t)|/|\rho_{2k'}(0)|)}{\log(|\rho_{1k}(t)|/|\rho_{1k}(0)|)} \quad (34)$$

for any k, k' , which theoretically will be time-independent. The value of R then determines the ratio of the decay rates. While both models agree qualitatively in their approach of the state of complete ignorance, the specific value of R acts as a fingerprint of the underlying processes described by a continuous Lindblad monitoring or discrete, iterated POVM measurements.

V. REPRESENTATIONS IN TERMS OF PHASE-SPACE QUASIPROBABILITY FUNCTIONS

To gain further insights into the decoherence effects of the Lindblad dynamics (1) and the POVM map (21), we consider the corresponding dynamical equation and the transformation rule satisfied by phase-space quasiprobability functions. To this end we shall be working with a parametric family of quasiprobability distributions for $SU(2)$ systems [46–49] defined by

$$F^\sigma(\theta, \phi) = \text{tr}(\hat{\rho} \hat{w}^\sigma(\theta, \phi)) \quad (35)$$

on the spherical phase space associated with a given quantum state $\hat{\rho}$. Here the Stratonovich-Weyl kernel

$$\hat{w}^\sigma(\theta, \phi) = a_J \sum_{L=0}^{2J} \sum_{k=-L}^L \left[\frac{\binom{2J}{L}}{\binom{2J+L+1}{L}} \right]^{-\frac{\sigma}{2}} Y_L^k(\theta, \phi) \hat{T}_{L,k}^J \quad (36)$$

satisfies the normalisation $\int \hat{w}^\sigma(\theta, \phi) d\mu_{\theta, \phi}^J = \mathbb{1}$ and the unit-trace condition $\text{tr}(\hat{w}^\sigma(\theta, \phi)) = 1$. Here we have defined $a_J = (2J+1)^{-1/2}$.

The normalisation of the kernel $\hat{w}^\sigma(\theta, \phi)$ implies that $\int F^\sigma(\theta, \phi) d\mu_{\theta, \phi}^J = 1$, but in general the positivity condition $F^\sigma(\theta, \phi) \geq 0$ is not satisfied. The family $\{F^\sigma\}$ includes, in particular, the Husimi Q function ($\sigma = -1$), which is manifestly positive [50], the Wigner-Stratonovich W function ($\sigma = 0$) [51], and the Glauber-Sudarshan P function ($\sigma = +1$) [52], for $SU(2)$ systems. The negativity of the quasiprobability distribution is progressively suppressed with decreasing σ .

While we can directly deduce the time-dependent phase-space distribution from the time-dependent density matrices derived in sections II and III, it is instructive to consider the dynamical equations for the phase

space distributions arising from the Lindblad dynamics (1). We will show that $F^\sigma(\theta, \phi, t)$ satisfies the heat equation on the sphere:

$$\frac{dF^\sigma}{dt} = \frac{\gamma}{2} \left(\frac{\partial^2}{\partial \theta^2} + \cot \theta \frac{\partial}{\partial \theta} + \frac{1}{\sin^2 \theta} \frac{\partial^2}{\partial \phi^2} \right) F^\sigma. \quad (37)$$

To derive (37), we use the self-adjointness of \mathcal{L} with respect to the Hilbert-Schmidt inner product to find

$$\partial_t F^\sigma = \text{tr}(\mathcal{L}(\hat{\rho}) \hat{w}^\sigma) = \text{tr}(\hat{\rho} \mathcal{L}(\hat{w}^\sigma)). \quad (38)$$

To evaluate $\mathcal{L}(\hat{w}^\sigma)$, note that \mathcal{L} acts only on the operator part $\hat{T}_{L,m}^J$ of each term in the sum (36). Hence on account of (15) we obtain

$$\begin{aligned} \mathcal{L}(\hat{w}^\sigma) &= a_J \sum_{L,k} \left[\frac{\binom{2J}{L}}{\binom{2J+L+1}{L}} \right]^{-\frac{\sigma}{2}} Y_L^k \mathcal{L}(\hat{T}_{L,k}^J) \\ &= \frac{\gamma}{2} a_J \sum_{L,k} \left[\frac{\binom{2J}{L}}{\binom{2J+L+1}{L}} \right]^{-\frac{\sigma}{2}} (-L(L+1)) Y_L^k \hat{T}_{L,k}^J. \end{aligned} \quad (39)$$

On the other hand, spherical harmonics, by definition, satisfy $\Delta_{\mathbb{S}^2} Y_L^k = -L(L+1) Y_L^k$, where

$$\Delta_{\mathbb{S}^2} = \frac{\partial^2}{\partial \theta^2} + \cot \theta \frac{\partial}{\partial \theta} + \frac{1}{\sin^2 \theta} \frac{\partial^2}{\partial \phi^2} \quad (40)$$

denotes the angular part of the Laplacian that appears in (37). Hence we deduce that

$$\mathcal{L}(\hat{w}^\sigma(\theta, \phi)) = \frac{\gamma}{2} \Delta_{\mathbb{S}^2} \hat{w}^\sigma(\theta, \phi), \quad (41)$$

from which it follows that

$$\begin{aligned} \partial_t F^\sigma &= \frac{\gamma}{2} \text{tr}(\hat{\rho} \Delta_{\mathbb{S}^2} \hat{w}^\sigma) \\ &= \frac{\gamma}{2} \Delta_{\mathbb{S}^2} \text{tr}(\hat{\rho} \hat{w}^\sigma) = \frac{\gamma}{2} \Delta_{\mathbb{S}^2} F^\sigma, \end{aligned} \quad (42)$$

and this establishes (37).

The solution to the heat equation (37) is found by eigenfunction expansion. Writing

$$F^\sigma(\theta, \phi, t) = a_J \sum_{L,k} g_{Lk}(t) \overline{Y_L^k(\theta, \phi)} \quad (43)$$

for some expansion coefficients g_{Lk} and substituting this in (37) gives $\partial_t g_{Lk} = -\frac{\gamma}{2} L(L+1) g_{Lk}$, so each coefficient decays exponentially according to $g_{Lk}(t) = e^{-\frac{\gamma}{2} L(L+1)t} g_{Lk}(0)$. The initial coefficients are determined by evaluating $F^\sigma(\theta, \phi, 0) = \text{tr}(\hat{\rho}(0) \hat{w}^\sigma)$ directly: substituting the expansion (13) into (35)–(36) and evaluating the trace using $\text{tr}(\hat{T}_{L,k}^J \hat{T}_{L',m}^J) = (-1)^k \delta_{LL'} \delta_{k,-m}$ together with $Y_L^{-k} = (-1)^k \overline{Y_L^k}$ gives $g_{Lk}(0) = \left(\frac{\binom{2J}{L}}{\binom{2J+L+1}{L}} \right)^{-\sigma/2} \rho_{Lk}(0)$, and hence we obtain the explicit solution

$$F^\sigma(\theta, \phi, t) = a_J \sum_{L,k} e^{-\frac{\gamma}{2} L(L+1)t} \left(\frac{\binom{2J}{L}}{\binom{2J+L+1}{L}} \right)^{-\frac{\sigma}{2}} \rho_{Lk}(0) \overline{Y_L^k(\theta, \phi)}. \quad (44)$$

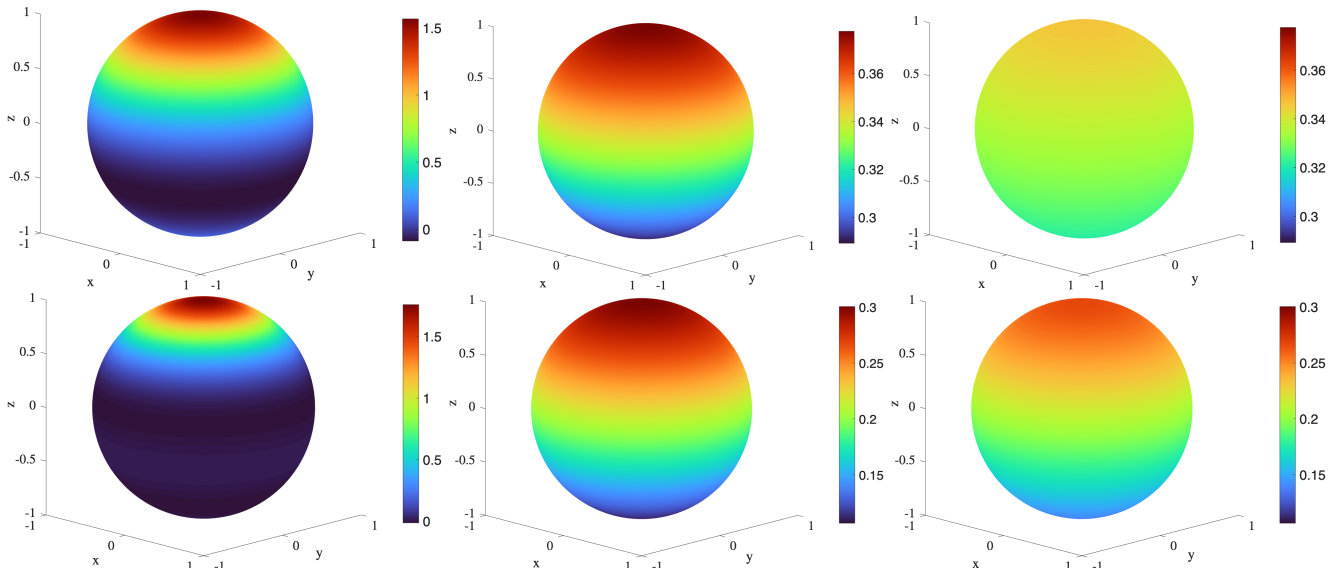


FIG. 2: Comparison of the decoherence models for an initial spin coherent state for $J = 1$ (top) and $J = 5$ (bottom). The left column shows the Wigner functions of initial coherent states with $J = 1$ and $J = 5$. The middle column shows the transformed Wigner functions after four iterations of POVM measurements. The right column shows the Wigner functions as the solution to the Lindblad evolution at time $t = 4$ (with $\gamma = 1/J$). The results illustrate the fact that features of a coherent state with higher spins are more robust against decoherence.

To express the solution for the quasidistribution function in terms of its initial condition, we use the orthogonality of spherical harmonics to deduce that

$$a_J \left(\frac{\binom{2J}{L}}{\binom{2J+L+1}{L}} \right)^{-\frac{\sigma}{2}} \rho_{Lk}(0) = \int Y_L^m(\theta, \phi) F^\sigma(\theta, \phi, 0) d\mu_{\theta, \phi}^0. \quad (45)$$

Substituting this in the right side of (44) we obtain

$$F^\sigma(\theta, \phi, t) = \sum_{L,k} e^{-\frac{\gamma}{2} L(L+1)t} \overline{Y_L^k(\theta, \phi)} \int Y_L^k(\theta', \phi') F^\sigma(\theta', \phi', 0) d\mu_{\theta', \phi'}^0. \quad (46)$$

Summing over k , and using the addition theorem for spherical harmonics, finally gives the expression

$$F^\sigma(\theta, \phi, t) = \sum_{L=0}^{2J} e^{-\frac{\gamma}{2} L(L+1)t} \int P_L(\cos \eta) F^\sigma(\theta', \phi', 0) d\mu_{\theta', \phi'}^L, \quad (47)$$

where $\cos \eta = \cos \theta \cos \theta' + \sin \theta \sin \theta' \cos(\phi - \phi')$ and

$$P_L(\cos \eta) = \sum_{k=-L}^L \frac{Y_L^k(\theta, \phi) \overline{Y_L^k(\theta', \phi')}}{2L+1} \quad (48)$$

is the L^{th} zonal harmonic [23].

The phase-space representation of the Lindblad equation thus shows that the dynamics give rise to a heat

equation associated with a Brownian motion on phase space, whose solution asymptotically converges to the uniform distribution $F^\sigma(\theta, \phi, t) \rightarrow (2J+1)^{-1}$ for all σ . This follows from (47), which shows that in the large time limit the only surviving term in the sum is the one for which $L = 0$, but we have $P_0 = 1$ and the normalisation condition $\int F^\sigma(\theta, \phi) d\mu_{\theta, \phi}^L = (2L+1)/(2J+1)$. Thus, irrespective of the value of σ , all Stratonovich-Weyl phase-space quasidistributions F^σ obey the same heat equation on the sphere.

Next, to gain insights into the phase-space characteristics of the POVM measurements, consider their impacts on the phase-space quasidistribution function F^σ . For the impact of the coherent-state POVM, the fact that the eigenvalues of Φ appear in the expression (36) of the Stratonovich-Weyl kernel shows at once that the action of each measurement is to lower the value of σ by 2. This follows from the identity that $\text{tr}(\Phi[\hat{\rho}]\hat{w}^\sigma) = \text{tr}(\hat{\rho}\Phi[\hat{w}^\sigma])$, on account of the self-adjointness of the phase-space measurement operation. Hence after performing a single phase-space measurement, the quasidistribution function transforms according to $F^\sigma \mapsto F^{\sigma-2}$. More generally, writing $F^\sigma(\theta, \phi, n)$ for the quasidistribution function resulting from n successive POVM measurements, we have

$$F^\sigma(\theta, \phi, n) = F^{\sigma-2n}(\theta, \phi, 0). \quad (49)$$

In Figure 2 we compare the behaviours of the state of the system as represented by the Wigner-Stratonovich function under the Lindblad dynamics and the POVM iteration for an initial coherent state of $J = 1$ and $J = 5$ spin systems. These correspond to the initial states used in Figure 1. Note the different colour scales used for the different plots. We remark on the observation that the

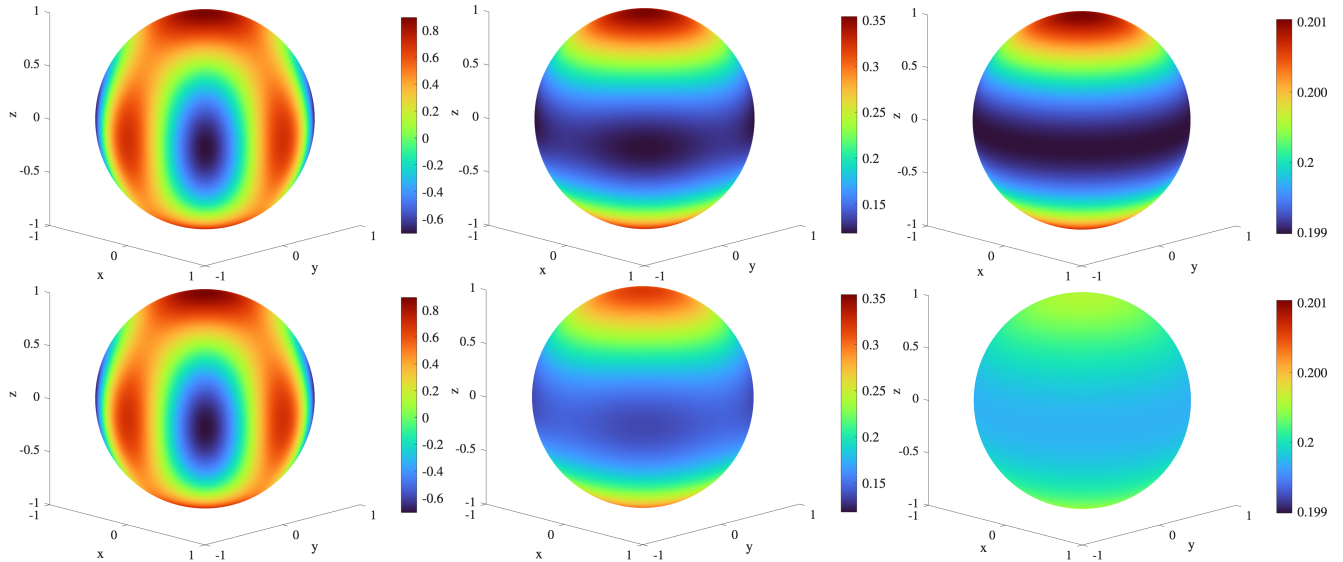


FIG. 3: Decoherence of the state $|\psi\rangle = \frac{1}{\sqrt{2}}(|m=J\rangle + |m=-J\rangle)$ with $J=2$. The top row represents the effect of POVM measurements after one (middle) and five (right) iterations. The bottom row shows the effect of Lindbladian dynamics at times $t=1$ and $t=5$ (with $\gamma=1/J$). The approach to uniform distribution resulting from decoherence is faster for the Lindblad dynamics in this example.

spin $J=5$ coherent state “decoheres” slower than the spin $J=1$ state in both POVM and Lindblad evolution, if we interpret decoherence as merely the decay of the matrix elements. Also note that while both dynamics asymptotically lead the state to the uniform distribution on the sphere, there are marked differences in the fluctuations between POVM and Lindblad evolution, where the Lindblad evolution washes out the features of the Wigner function faster than the POVM iterations. These differences are, as expected, more pronounced for the smaller value of J .

To contrast the impact of decoherence on an initial coherent state, in Figure 3 we take a highly quantum initial state

$$|\psi\rangle = \frac{1}{\sqrt{2}}(|m=J\rangle + |m=-J\rangle) \quad (50)$$

and compare the effect of the two decoherence models on this state. Here, the left column shows the Wigner function of the initial state (they are identical). In the middle and the right columns, the top row shows the resulting Wigner function under the POVM iterations (for $n=1,5$), while the bottom row shows the solution to the Lindblad equation with $\gamma=1/J$ at $t=1,5$. Once the interference fringes are washed out, the application of POVM measurements appears to keep the structure of the Wigner function. Note, however, that the colour scales are changing, indicating an approach to a uniform distribution while keeping the structure. Under the Lindbladian dynamics (bottom row), on the other hand, the approach to uniformity is more pronounced.

VI. DECOHERENCE TIMESCALE AND POSITIVITY OF THE WIGNER FUNCTION

In the context of phase-space representations, the positivity of the quasidistribution function is often considered in the literature. One reason for the interest on positivity is that if F^σ for $\sigma=+1$, the Glauber-Sudarshan P function, is nonnegative, then the state $\hat{\rho}$ is often viewed as being classical [53]. On the other hand, we recall that the quasidistribution function for $\sigma=-1$ is the Husimi density, which is strictly nonnegative. It follows from (49) that for any value of σ , the quasidistribution function is transformed into a positive density function after applying at most $\lceil(\sigma+1)/2\rceil$ iterations of phase-space measurements. (See [54] for an analogous analysis on tomographic decoherence models.) This provides a sharp upper bound on the number of measurements required to guarantee transition into classicality, if classicality were to be interpreted as the positivity of a given quasidistribution function.

An analogous question on the positivity of F^σ can be addressed under the Lindblad dynamics (1), as discussed also in [17]. Here we remark that for $J=1/2$, owing to the equivalence of the two decoherence models, we are able to give an exact time at which a given quasidistribution function becomes positive. This follows on account of the fact that the solution to the Lindblad dynamics (1) agrees with the resulting state after n iterations of the POVM measurements at times

$$t_n = \frac{\log 3}{\gamma} n. \quad (51)$$

It follows that for $J=1/2$ and any σ , the quasidistribution function becomes positive under the Lindblad dy-

namics at time

$$t_\sigma^* = \frac{\log 3}{\gamma} [(\sigma + 1)/2], \quad (52)$$

which is an exact result. For $J > 1/2$ we do not have an exact result, but it seems reasonable to conjecture that positivity is ensured provided that the damped σ kernel in (44), due to decoherence, becomes no sharper than the Husimi ($\sigma = -1$) kernel. That is, if

$$e^{-\frac{1}{2}\gamma L(L+1)} \left(\frac{\binom{2J}{L}}{\binom{2J+L+1}{L}} \right)^{-\frac{\sigma}{2}} \leq \left(\frac{\binom{2J}{L}}{\binom{2J+L+1}{L}} \right)^{\frac{1}{2}} \quad (53)$$

for all L , then we restore positivity. Now the largest value the binomial ratio can take is for $L = 2J$, so solving this for t we find that

$$t_\sigma^* = \frac{\sigma + 1}{2\gamma J(2J + 1)} \log \binom{4J + 1}{2J}. \quad (54)$$

In particular, for $J \gg 1$ this gives

$$t_\sigma^* \approx \frac{\sigma + 1}{4\gamma J^2} (4J \log 2 - \frac{1}{2} \log(2\pi J)). \quad (55)$$

This result suggests that if γ is held fixed for different J , then for larger spins the positivity is attained faster, according to $t_\sigma^* \sim 1/J$. On the other hand, should γ scale like $\gamma = 1/J$, then we have $t_\sigma^* \approx (\sigma + 1) \log 2$.

VII. SUMMARY AND DISCUSSION

In summary, we have presented two models for phase-space decoherence of spin systems, one based on a homogeneous spin dephasing induced by the Lindblad dynamics, and one based on the phase-space POVM measurements. We have shown that for $J > 1/2$ the associated decoherence rates are not in agreement, although the qualitative behaviours of the system implied by the two decoherence models are very similar and the discrepancy rapidly disappears in increasing J . We found, perhaps not surprisingly, that a coherent state with an increasing J becomes more robust against phase-space decoherence. We have also compared the two decoherence models in terms of the phase-space quasidistribution functions, and provided estimates for the first passage times for their positivity.

In this connection it is worth drawing attention to the fact that there are two different timescales that emerge, namely, the timescale for the decay of the elements of the density matrix, and the timescale for recovering the positivity of the quasiprobability distributions. Traditionally, decoherence is viewed as the decay effect of the elements of the density matrix, and here we find that the decay rates are smaller for larger spins. On the other hand, decoherence is often viewed as the signature for the emergence of classicality, but so is the positivity and the

disappearance of interference fringes in the quasiprobability distributions [55]. However, for the latter, the timescale is smaller for larger spins, which is the opposite of the decay rate analysis. Hence depending on which criterion (decay of the density matrix or the positivity of the quasiprobability distribution) one chooses, the answer to the question whether systems with larger spins classicalise faster differs.

Acknowledgements

RM acknowledges support through an Imperial College President's PhD Scholarship.

Appendix A: Microscopic derivation of the Lindblad equation (1)

If three independent components of the spin or angular momentum of a particle are randomly monitored by the environment, then we may model the interaction between the system, whose state at time t is given by $\hat{\rho}_t$, with its environment over the time period $[t, t + dt]$ through a unitary operator by writing

$$\hat{\rho}_t + d\hat{\rho}_t = e^{-i\sqrt{\gamma}(\hat{J}_x w_t^x + \hat{J}_y w_t^y + \hat{J}_z w_t^z)} dt \times \hat{\rho}_t e^{i\sqrt{\gamma}(\hat{J}_x w_t^x + \hat{J}_y w_t^y + \hat{J}_z w_t^z)} dt \quad (A1)$$

for an infinitesimal modification of the state over a short time period dt . Here, we represent the three independent components of the angular momentum by the operators $\{\hat{J}_x, \hat{J}_y, \hat{J}_z\}$, and we use a bold font $d\hat{\rho}_t$ for the state transformation to highlight the fact that it is a random perturbation that will have to be averaged to recover the density matrix. The interaction with the environment, however, is highly oscillatory and is thus random, and we model this by use of three statistically-independent Gaussian white noise terms $\{w_t^x, w_t^y, w_t^z\}$. We let $\sqrt{\gamma}$ model the coupling strength. In essence, our microscopic model takes the form of the Peres model for the system-environment interaction for the monitoring of the system [56]. For $dt \ll 1$ we expand (A1) to obtain

$$\hat{\rho}_t + d\hat{\rho}_t = \left(1 - i\sqrt{\gamma}(\hat{\mathbf{J}} \cdot \mathbf{w}_t)dt - \frac{1}{2}\gamma(\hat{\mathbf{J}} \cdot \mathbf{w}_t)^2(dt)^2 \right) \hat{\rho}_t \times \left(1 + i\sqrt{\gamma}(\hat{\mathbf{J}} \cdot \mathbf{w}_t)dt - \frac{1}{2}\gamma(\hat{\mathbf{J}} \cdot \mathbf{w}_t)^2(dt)^2 \right), \quad (A2)$$

where we have written $\hat{\mathbf{J}} \cdot \mathbf{w}_t$ for $\hat{J}_x w_t^x + \hat{J}_y w_t^y + \hat{J}_z w_t^z$. Expanding the right side of (A2), making use of the property $(w_t dt)^2 = dt$ of the Gaussian white noise [57], and taking the average of the resulting expression for $d\hat{\rho}_t$, noting that independent Gaussian white noise terms have vanishing expectations, and writing $d\hat{\rho}_t = \mathbb{E}[d\hat{\rho}_t]$ for the expectation, we deduce the Lindblad equation (1).

-
- [1] Brody D. C., Graefe E.-M., and Melanathuru R. 2025 Phase-space measurements, decoherence, and classicality. *Physical Review Letters* **134**, 120201.
- [2] Zurek, W. H. 2002 Decoherence and the Transition from Quantum to Classical—Revisited. *Los Alamos Science* **27**,2–25.
- [3] Joos E., Zeh H. D., Kiefer C., Giulini D., Kupsch J. and Stamatescu I. O. 2003 *Decoherence and the Appearance of a Classical World in Quantum Theory* 2nd ed. (Berlin: Springer)
- [4] Zurek W. H. 2022 Quantum theory of the classical: einselection, envariance, quantum Darwinism and extantons. *Entropy* **24**,1520.
- [5] Schlosshauer M. 2010 *Decoherence and the Quantum-to-Classical Transition*. (Berlin: Springer)
- [6] Davidovich L. 1999 Decoherence, Wigner Functions, and the Classical Limit of Quantum Mechanics in Cavity QED. *AIP Conference Proceedings* **461**, 151–162.
- [7] Zurek W. H. 2001 Sub-Planck structure in phase space and its relevance for quantum decoherence. *Nature***412**, 712–717.
- [8] Murakami M., Ford G. W. and O’Connell R. F. 2003 Decoherence in phase space. *Laser Physics* **13**, 180–183.
- [9] Ozorio de Almeida A. 2003 Decoherence of semiclassical Wigner functions. *Journal of Physics A: Mathematical and General* **36**, 67–86.
- [10] Kossakowski A. 1972 On quantum statistical mechanics of non-Hamiltonian systems. *Reports on Mathematical Physics* **3**, 247–274.
- [11] Lindblad G. 1976 On the generators of quantum dynamical semigroups. *Communications in Mathematical Physics* **48**, 119–130.
- [12] Gorini V., Kossakowski A., and Sudarshan E. C. G. 1976 Completely positive dynamical semigroups of N-level systems. *Journal of Mathematical Physics* **17**,821–825.
- [13] Hertz A. and De Bièvre S. 2020 Quadrature coherence scale driven fast decoherence of bosonic quantum field states. *Physical Review Letters* **124**,090402.
- [14] De Bièvre S., Horoshko D. B., Patera G., and Kolobov M. I. 2019 Measuring nonclassicality of bosonic field quantum states via operator ordering sensitivity. *Physical Review Letters* **122**, 080402.
- [15] Hall B. C. 1994 The Segal–Bargmann “coherent state” transform for compact Lie groups. *Journal of Functional Analysis* **122**,103–151.
- [16] Rivas, Á. and Luis, A. 2013 SU(2)-invariant depolarization of quantum states of light. *Phys. Rev. A***88**, 052120.
- [17] Denis, J. and Martin, J. 2022 Extreme depolarization for any spin. *Phys. Rev. Res.* **4**, 013178.
- [18] Tidström, J. and Sjöqvist, E. 2003 Uhlmann’s geometric phase in presence of isotropic decoherence. *Phys. Rev. A***67**, 032110.
- [19] Klimov, A. B., Romero, J. L. and Sánchez Soto, L. L. 2006 Single quantum model for light depolarization. *J. Opt. Soc. Am. B***23**, 126.
- [20] Arsenijević, M., Jeknić-Dugić, J. and Dugić, M. 2017 Generalized Kraus operators for the one-qubit depolarizing quantum channel. *Braz. J. Phys.* **47**, 339.
- [21] Varshalovich D. A., Moskalev A. N., and Khersonskii V. K. 1998. *Quantum Theory of Angular Momentum* (World Scientific).
- [22] Racah G. 1942 Theory of Complex Spectra. II. *Physical Review* **62**, 438–462.
- [23] Edmonds A. R. 1996. *Angular Momentum in Quantum Mechanics*. (Princeton University Press).
- [24] Varshalovich, D. A., Moskalev, A. N. and Khersonskii, V. K. 1988. *Quantum Theory of Angular Momentum* (Singapore: World Scientific Publishing).
- [25] Karl Blum 1996. *Density Matrix Theory and Applications* (New York: Springer)
- [26] Appleby D. M. 2000 Optimal measurements of spin direction. *International Journal of Theoretical Physics* **39**, 2231–2252.
- [27] Weigert S. and Busch P. 2003 Lüders theorem for coherent-state POVMs. *Journal of Mathematical Physics* **44**, 5474–5486.
- [28] Radcliffe M. J. 1971 Some properties of coherent spin states. *Journal of Physics A: General Physics* **4**, 313–323.
- [29] Arecchi T. F., Courtens E., Gilmore R. and Thomas H. 1972 Atomic coherent states in quantum optics *Physical Review A* **6**,2211.
- [30] Perelomov A. 1986 *Generalized Coherent States and Their Applications*. (Springer-Verlag).
- [31] Zhang W.-M., Feng D. H. and Gilmore R. 1990 Coherent states: Theory and some applications. *Reviews of Modern Physics* **62**, 867–927.
- [32] Ali, S. T., Antoine, J.-P. & Gazeau, J.-P. 2013 *Coherent States, Wavelets, and Their Generalizations*. (Berlin: Springer).
- [33] Brody D. C. and Graefe, E. M. 2010 Coherent states and rational surfaces. *Journal of Physics A: General Physics* **43**, 255205.
- [34] Brody D. C. and Hughston L. P. 2021 Quantum measurement of space-time events. *Journal of Physics A* **54**, 235304.
- [35] Brody D. C. and Hughston L. P. 2015 Universal quantum measurements. *Journal of Physics: Conference Series* **624**, 012002.
- [36] Klimov A. B. and Chumakov S. M. 2009 *A Group-Theoretical Approach to Quantum Optics: Models of Atom-Field Interactions* (Wiley-VCH).
- [37] Biedenharn L. C., Louck J. D., and Carruthers P. A. 1984 *Angular Momentum in Quantum Physics: Theory and Application*.
- [38] Rose E. M. 1995 *Elementary Theory of Angular Momentum* (Courier Corporation).
- [39] Cohen-Tannoudji C., Diu B., and Laloë F. 1986 *Quantum Mechanics* (Hermann).
- [40] Budker D., Kimball D. F. and DeMille D. P. 2002 Optical magnetometry. *Reviews of Modern Physics* **74**, 1153–1201.
- [41] Rochester S. M. and Budker D. 2001 Nonlinear magneto-optical rotation with frequency-modulated light in the geophysical field range. *American Journal of Physics* **69**, 450–454.
- [42] Geremia J. M., Stockton J. K. and Mabuchi H. 2005 Suppression of spin projection noise in broadband atomic magnetometry. *Physical Review Letters* **94**, 203002.
- [43] Sewell R. J., Koschorreck M., Napolitano M., Dubost B., Behbood N. and Mitchell M. W. 2012 Magnetic sensitivity beyond the projection noise limit by spin squeezing.

- Physical Review Letters* **109**,253605.
- [44] Rochester S. M., Ledbetter M. P., Zigdon T., Wilson-Gordon A. D. and Budker D. 2012 Orientation-to-alignment conversion and spin squeezing. *Physical Review A* **85**, 022125.
- [45] Stahovich J. T., Rowe B. A., Huennekens J., Lyyra A. M. and Ahmed E. H. 2024 Molecular angular momentum orientation using dressed states created by laser radiation. *Physical Review A* **110**, 063101.
- [46] Stratonovich H. L. 1955 On distributions in representation space. *Soviet Physics JETP* **4**, 891–898.
- [47] Klimov A. B., Romero J. L. and De Guise H. 2017 Generalized SU(2) covariant Wigner functions and some of their applications. *Journal of Physics A: Mathematical and Theoretical* **50**, 323001.
- [48] Klimov A. B. 2002 Exact evolution equations for SU(2) quasidistribution functions. *Journal of Mathematical Physics* **43**, 2202-2213.
- [49] Klimov A. B. and Chumakov S. M. 2002 On the SU(2) Wigner function dynamics. *Revista Mexicana de Física* **48**, 317-324.
- [50] Husimi, K. 1940 Some formal properties of the density matrix. *Proceedings of the Physico-Mathematical Society of Japan* **22**, 264–314.
- [51] Wigner, E. P. 1932 On the quantum correction for thermodynamic equilibrium. *Physical Review* **40**, 749–759.
- [52] Sudarshan E. C. G. 1963 Equivalence of semiclassical and quantum mechanical descriptions of statistical light beams. *Physical Review Letters* **10**, 277–279.
- [53] Giraud, O., Braun, P. and Braun, D. 2008 Classicality of spin states. *Phys. Rev.* **A78**, 042112.
- [54] Brody, D. C. and Melanathuru R. 2026 Decoherence from universal tomographic measurements. *Physical Review Research* **8**, L012042.
- [55] Davis J., Kumari M., Mann R. B., and Ghose S. 2021 Wigner negativity in spin- j systems. *Physical Review Research* **3**,033134.
- [56] Peres, A. 2000 Classical interventions in quantum systems. I. The measuring process. *Phys. Rev.* **A61**, 022116.
- [57] Hida, T. 1976 Analysis of Brownian functionals. *Mathematical Programming Study* **5**, 53-59.